Original Paper

Modeling of the aging of glass furnace regenerators[1])

Ruud G. C. Beerkens and Hendrikus P. H. Muysenberg
TNO Institute of Applied Physics, Eindhoven (The Netherlands)

Hansjürgen Barklage-Hilgefort[2])
Hüttentechnische Vereinigung der Deutschen Glasindustrie (HVG), Frankfurt/M. (FRG)

A model has been developed to predict the decrease of the thermal performance of glass furnace regenerators due to fouling by flue gas condensates. The model consists of four parts:

a) description of the thermal performance (heat transfer) of regenerator checkers;

b) description of the heat transfer in the furnace combustion chamber;

c) determination of volatilization of sulfur, chloride and sodium components from the melt;

d) modeling of chemical reactions in and deposition from flue gases in the regenerator.

The aging and the reduction of the thermal efficiency due to fouling has been predicted:

- for different checkerwork constructions or refractory types;
- as a function of pull rate;
- as a function of glass melt temperatures;
- as a function of applied cullet fraction.

Depending on the different conditions, the predicted increase in energy consumption is about 1 up to more than 3 %/year, mainly due to fouling. Cruciform and chimney block checkers seem to be less sensitive for this fouling than basketweave packings. As molten glass temperatures increase, dust emissions and fouling rates are going up. According to the model calculations, a higher cullet fraction in the batch will lead to reduced aging rates of the regenerators. The model is in quite good agreement with practical observations in industrial furnaces.

Modell für die Alterung der Regeneratoren von Glasschmelzöfen

Ein erweitertes Rechenmodell für die Abschätzung bzw. Vorhersage von Änderungen des thermischen Verhaltens von Regeneratoren durch Ablagerungen aus den Ofenabgasen wurde entwickelt. Das Modell besteht aus vier Untermodellen:

a) Beschreibung der Wärmeübertragung in der Regeneratorpackung;

b) Beschreibung der Wärmeübertragung im Oberofen;

c) Abschätzung der Verdampfungsraten für Schwefel-, Chlorid- und Natriumverbindungen aus dem Gemengeteppich und aus der Glasschmelze;

d) Modellierung chemischer Reaktionen in und von Ablagerungen aus Abgasen in den Regeneratoren.

Die Alterung und die Abnahme des wärmetechnischen Wirkungsgrades durch Ablagerungen werden mit Hilfe des kombinierten Modells berechnet:

- für verschiedene Setzweisen oder Steinarten;
- abhängig von der Glasschmelzleistung;
- abhängig von den Glasschmelztemperaturen;
- abhängig vom Scherbenanteil im Gemenge.

Sowohl aus der Praxis als auch aus den Berechnungen geht hervor, daß die Alterung des Ofens eine Erhöhung des spezifischen Energieverbrauches von 1 bis 3 % pro Jahr zur Folge haben kann. Diese wird überwiegend hervorgerufen durch Regeneratorablagerungen. Kreuzstein- und Topfsteingitterungen sind dabei weniger empfindlich für diese Ablagerungen als Märzgitterarten. Die Staubbildung und Alterung des Regenerators nehmen wesentlich zu bei Erhöhung der Temperatur der Glasschmelze, aber nehmen ab bei einer Zunahme des Scherbenanteiles im Gemenge. Die Modellergebnisse stimmen im allgemeinen gut mit praktischen Erfahrungen aus der Glasindustrie überein.

1. Introduction

Glass furnace lifetimes have been considerably increased over the last fifty years. Improved refractory materials and optimized process control contributed to a decrease in corrosion rates. However, during the furnace lifetimes, the specific energy consumption generally increases from 5 to more than 15 % [1]. This is not only caused by increasing air leakages, attack of refractory materials and insulation but mainly by the fouling of regenerators by condensation products from the flue gases. The composition of the deposition layers depends very much on

Received May 18, 1992.

[1]) Paper presented in German at the HVG/NCNG Colloquium "Modelling of Glass Processing" on November 6, 1991 in Maastricht (The Netherlands).

[2]) Now with: Nienburger Glas GmbH, Nienburg (FRG).

the composition of the molten glass and on the position in the regenerator. In lead glass furnaces lead oxides and in borosilicate glass furnaces often alkali borates condense from the flue gases. In soda–lime–silica glass furnaces, these condensates contain mainly 80 to 95 % sodium sulfates. Sodium components vaporize from the molten glass mainly by reaction of the sodium oxide in the melt with water vapor in the furnace atmosphere, leading to the formation of volatile sodium hydroxides.

Sulfur dioxide formed by the sulfur in the fuel or by decomposition of sulfates in the melt reacts with sodium hydroxide at temperatures below 1100 to 1250 °C. This leads to condensation of sodium sulfates in the regenerator packings. The sodium sulfate condensation takes place at the surface of the colder regenerator bricks. This causes deposition of liquid sodium sulfate above 884 °C and fouling by crystalline material below this temperature. In the lower and cooler regenerator sections, sodium sulfate dust will be formed, this dust partly sticks at the refractory surfaces.

Generally, the deposition products have a lower thermal conductivity than the refractories, the heat transfer from flue gases to the bricks will be reduced by these insulating deposition layers. After the reversal in the combustion cycle, the heat release by the preheated packings to the air is also limited by the insulating salt layers. Apart from the reduction of the thermal conductivity by the deposition process, sodium sulfate may cause severe damages by corrosion or mechanical attack during sublimation processes.

The fouling by salt deposits depends very much on the concentrations of the sodium compounds and sulfur oxides in the flue gases entering the regenerator chambers. The volatilization from the batch blanket and the molten glass determines the concentration levels of sodium compounds in the flue gases. The sulfur oxide sources are the sulfate in the batch and the sulfur in the fuels. The values of the flue gas temperatures and concentrations of volatilization products at the entrance of the regenerator chamber are very important for the calculation of the fouling and thermal behavior of regenerators during the furnace lifetime.

The flue gas composition and temperatures are governed by the processes in the furnace: combustion, radiative heat transfer and volatilization from the batch blanket and the melt.

In sections 2. to 5. four submodels for the description of the thermal behavior of regenerators, heat transfer in the furnace, deposition of salt layers, and volatilization will be briefly presented. Examples of calculation results for several process conditions and different regenerator checkerworks will be given in section 7.

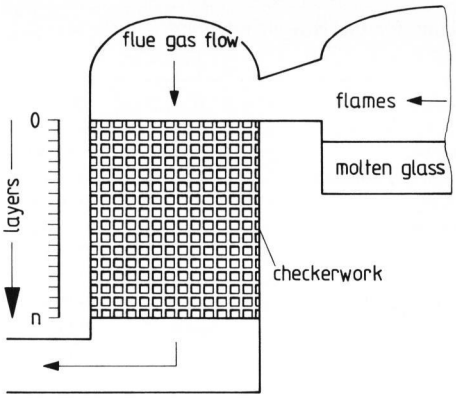

Figure 1. Scheme of a regenerator divided into layers for calculation procedure.

2. Regenerator heat transfer model

The modeling of the thermal performance of new regenerators has been developed by Barklage-Hilgefort [2]. His method is based on a numerical difference method in which the elementary heat transfer processes in the regenerator checkers are mathematically simulated.

Figure 1 shows a scheme of a regenerator. The calculation process acts as follows: The regenerator packing is divided into a certain number of layers, starting from the flue gas entrance in the direction of the flow of these flue gases. The total heat-transferring surface area of the checkers, the heat capacity and thermal conductivity depend on the structure and dimensions of the packings and the refractories which have been used. The checkerworks may consist of different sections with different packing arrangements.

In the calculation procedure, first a certain not necessarily realistic temperature distribution for the checkers is assumed. The temperature decrease of the flue gases flowing through the regenerator will be calculated per layer and per short time period Δt. The increase of the temperature of the refractories will be calculated also after this Δt. This procedure will be repeated for the next Δt period and again the temperature decrease of the flue gases and the temperature change of the refractories during this time step are determined per layer.

After one half of the regenerator cycle period, in which the regenerator has been heated by the flue gases, these calculations will be continued, now for cold air entering the regenerator at the former flue gas exit. The air will be preheated per layer and the refractory materials will be cooled down by this process. After this air-preheating half cycle, the calculation continues again for the situation of the regenerator being heated up by flue gases. The calculation process will be carried out until the exit temperatures of the flue gases and air remain constant for the next cycles.

Table 1. Coefficients for the Nusselt relation: $Nu = A + B \cdot Re$

checker configuration	A	B
smooth plain packing	7.8	0.0060
diagonally staggered pigeonhole	16.3	0.01135
basketweave packing	10	0.00713
pigeonhole checkerwork	13	0.00720
staggered packing	16.3	0.01135
cruciform packing	11.5	0.00820
corrugated cruciform packing	14.95	0.01066
chimney blocks	10.0	0.00713
chimney blocks TL	12.0	0.00713

A very important step in this calculation procedure is the heat transfer from the flue gases to the refractory materials, and, moreover, the heat transfer to the air [3], which mainly determines the thermal efficiency of the regenerator system.

At a certain moment and a certain position (layer) the heat flux, Q_s, is given by:

$$Q_s = \alpha \cdot (T_{fi}(t_j) - T_{rsi}(t_j)) \,. \tag{1}$$

According to Hausen [4], $T_{rsi}(t_j)$ can be replaced by the time-dependent average brick temperature and Q_s can be calculated as:

$$Q_s = \alpha \cdot (T_{fi}(t_j) - T_{rci}(t_j))/(1 - \gamma(t_j) \cdot \alpha) \,. \tag{2}$$

The function $\gamma(t_j)$ depends on the dimensions of the refractory materials and the heat capacity and conductivity of this material. This function can be calculated separately for every time and per layer using Hausen's [4] approximations. By this procedure the heat transfer can be calculated quite accurately and fast. The accuracy can be improved by using not only the temperatures of the gas and refractory at the beginning of a period of time Δt and at the entrance of layer i, but by using a linear approximation for the temperature decrease or increase of the flue gases and the refractory materials in this layer during a period Δt and within the layer i. This results in the following corrected equation describing the average heat transfer in layer i:

$$Q_s = \frac{\alpha \cdot (T_{fi}(t_j) - T_{rci}(t_j))}{1 - \alpha \cdot \left[\gamma_i(t_j) - \left(\frac{\Delta F_s}{\dot{V}\, C_{pg}} + 2\,\frac{\Delta t}{\delta_r\, C_{pr}}\right)/2\right]} \,. \tag{3}$$

The convective heat transfer coefficients are derived using simple Nusselt number relations.

$$Nu = A + B \cdot Re \,. \tag{4}$$

A and B are empirically derived coefficients depending on the kind of checkers, and listed in table 1 [5]. From these Nusselt numbers the heat transfer coefficient can be determined for convective heat transfer. This heat transfer coefficient is corrected for radiative contributions in the very hot regions, depending on water vapor and carbon dioxide concentrations in the flue gases.

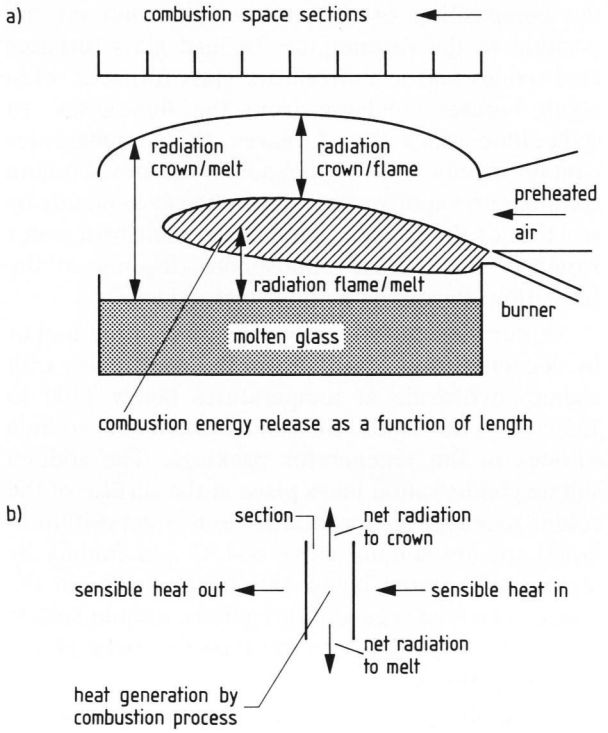

Figures 2a and b. Model of combustion chamber of a glass furnace; a) combustion space divided into sections, b) energy balance per section.

3. Combustion chamber model

The regenerator heat transfer model needs values for the flue gas temperatures, flue gas compositions and flue gas flows at the entrance of the regenerator. These depend on the combustion process, the energy consumption in the furnace and the radiative heat transfer between flames, the crown and the molten glass. Convection plays a minor role in the heat transfer process to the glass melt in the glass furnace combustion space [6]. The flue gas composition and the time-dependent flue gas temperature are used in the regenerator model. The flue gas temperature depends on the air-preheating temperature, determined by the regenerator model and the radiative heat transfer from the flames to the crown and to the surface of the molten glass. Figure 2 presents the most important processes.

For the derivation of these flue gas parameters, a relatively simple combustion chamber model has been developed. The heat transfer in the furnace combustion chamber by convection differs only by a few percent from the radiative heat transfer and is neglected in this submodel.

Schematically the calculation process for the radiative heat transfer consists of the following steps:

a) The combustion chamber along the combustion path is divided into ten or twenty segments. Initially, a first approach for the temperature profiles of the crown and the flame has to be assumed.

b) A certain empirical function is assumed for the burning process, which gives the amount of combustion energy generated in each segment.

c) Per segment a thermal balance is calculated: The total heat input by the gas flow entering the segment and the combustion energy are used for: the radiation to the superstructure and the molten glass surface, and for the flue gas heat contents leaving this segment. The model is able to take a certain recirculation of flue gases in the combustion chamber into account, using an empirical recirculation factor. Every segment is assumed to be an ideal mixer. The radiative emission considers the radiation from the flames to the molten glass and reverse, from the flames to the crown and reverse and from the crown to the molten glass and reverse. The calculation has to be carried out iteratively: Temperatures of the superstructure and the flame (layer of gas) are adjusted until these values remain constant and until the heat balances per segment are correct. The molten glass surface temperature will be assumed to have a certain fixed value which depends on the required glass quality. The emissivity is calculated as a function of gas layer or flame thickness, flame temperature and flame composition [6].

The radiation is assumed as to be gray. In reality the radiation depends very much on the wavelength. Carbon dioxide and water vapors radiate at certain spectral bands. The spectral selective emissivity depends also on temperature and the presence of soot particles in the flames. In addition to the energy transfer to the crown, the molten glass and the batch blanket, some extra energy losses have to be considered, like leakages of the furnace, radiation through these leakages and the forced cooling of the metal line by air. In the model, constant values for these losses have to be assumed.

The combustion chamber model and the regenerator heat transfer model are combined: The values for the air-preheating temperature and air flow rate calculated by the regenerator heat transfer model are necessary for the calculations with the combustion chamber model. On the other hand, the values for the temperatures, the compositions and the volumetric flows of the gases leaving the furnace are used for the regenerator model.

4. Volatilization model

The fouling of a regenerator depends on the condensation of volatilization products originating from the melt or batch blanket. In soda–lime–silica glass furnaces, sodium components vaporize partly from the batch blanket but mainly from the molten glass surface. These volatile sodium compounds react in the flue gases with sulfur oxides during the cooling process, leading to sodium sulfate formation below about 1250 °C. The sodium sulfate gas will condense below approximately 1100 °C; this results in dust/droplet formation or salt deposition. The condensation and deposition of sodium sulfate is a process which determines the fouling of regenerators and therefore, the reduction of the thermal efficiency of older regenerators: the aging process.

The concentrations of sodium compounds in the flue gases are mainly important for the deposition processes, but the sulfur oxide concentrations and to some extent the chloride concentrations also play a role in the chemistry here [7 and 8]. In lead glass furnaces, often alkali compounds vaporize together with lead oxides, leading to the deposition of sodium, potassium and lead salts or oxides. The deposition products in borosilicate glass furnaces appear to be often alkali borates ($NaBO_2$ or $Na_2B_4O_7$). Here the attention is focused on soda–lime–silica glass melting.

4.1. Sodium volatilization

Sodium components are entrained in the combustion gases by:

- carry-over of light soda particles:
- sodium chloride volatilization from the batch blanket; sodium chloride is an impurity in synthetic soda;
- sodium oxide reactions at the melt surface with the water vapor, leading to formation of volatile sodium hydroxides;
- sodium sulfate volatilization from the molten glass in gas bubbles, during the primary fining process.

The model takes into account:

a) the carry-over, dependent on the density of the soda used: The carry-over from light soda is assumed to be twice the carry-over from dense soda;

b) the fraction of cullet: The soda carry-over is given as milligram carry-over per kilogram of glass molten from primary raw materials.

The sodium chloride volatilization is assumed to be proportional to the soda concentration in the batch and to the concentration of the sodium chloride impurities in the synthetic soda.

The sodium hydroxide formation appears to be most important for the sodium volatilization. Figure 3 schematically shows this volatilization process at the molten glass surface. Conradt's model [9] has been used to describe this volatilization process. The sodium volatilization depends mainly on the molten

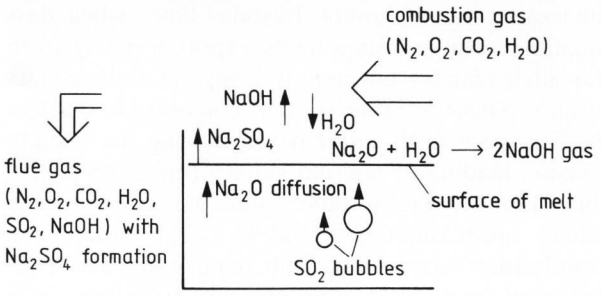

Figure 3. Volatilization of sodium components from the glassmelt surface.

glass surface temperature, the sodium oxide concentration in the melt, the flue gas velocity above the melt, and the water vapor concentration in the combustion products. Sodium sulfate volatilization is of minor importance, calculations using Conradt's model for vaporization at the molten glass surface and estimations for sodium sulfate diffusion into bubbles show that sodium sulfate vaporization contributes only 1 % or less to the sodium entrainment in the combustion gases.

4.2. Sulfur oxides in flue gases

The main sources for sulfur are the fuel, sulfate additions in the batch, sulfur impurities in the raw materials and sulfur in the cullet. In the model all the sulfur from the fuel is assumed to be converted into sulfur dioxide gas.

The total sulfur retention in the glass depends very much on the final glass color and the redox state [10]. In the model it has been assumed that flint or float glass contains 0.05 to 0.07 wt% sulfur, green or emerald green glass has a concentration of about 0.04 wt% sulfur and in light amber soda–lime–silica glass about 0.02 wt% will be dissolved. In dark amber glass the concentration of sulfur can reach values above 0.07 wt%.

The difference between the total sulfur input by fuel, sulfates and sulfides in the cullet minus the sulfur output by the glass has been assumed to be released as SO_2, which will be emitted by the flue gases or which will react with sodium compounds into sodium sulfates.

4.3. Chlorides in flue gases

The main chloride sources are synthetic soda and cullet. The chloride impurities in the soda appear to be much more volatile than in the glass. In this model only the chloride vaporization from the soda in the batch blanket has been considered. The chloride volatilization per kilogram glass has been assumed to be proportional to the soda content in the batch and the chloride concentration in the soda.

From the volatilization rates or formation rates of gaseous sodium, sulfur and chloride compounds, the concentrations of these components in the flue gases entering the regenerator chambers can be determined directly.

5. Deposition of sodium sulfate in the regenerator checkerworks

The deposition by condensation at the relatively cold surfaces in the checkers has been described in [7 and 8]. During the cooling of the flue gases in the regenerator, from about 1400 down to 500 °C, chemical reactions between the different flue gas components take place. The chemistry depends very much on the composition and the temperature of the flue gases; for furnaces producing sulfate-refined soda–lime–silica glasses, the formation of sodium sulfate from sodium chloride, sodium hydroxides and sulfur oxides causes condensation of this salt.

Condensation reactions occur at the surfaces of the checker bricks; deposition rates are determined by the diffusion of sodium and sulfur compounds from the flue gases through a diffusion boundary layer towards the brick surfaces. The most important diffusing components are: NaOH, Na, NaCl, HCl, SO_2, SO_3. The calculation process consists of:

a) Calculation of the thermodynamic equilibrium composition of the flue gases at the entrance of the regenerator;

b) Calculation of equilibrium flue gas composition in the first layer (top layer of the regenerator);

c) Calculation of the equilibrium flue gas composition at positions directly in contact with the surface of the regenerator bricks, first assuming a certain total sodium, sulfur and chloride concentration at these locations;

d) Calculation of the diffusion of all sodium, sulfur and chloride compounds through the flue gas boundary layer at the brick surfaces, using diffusivities, concentration differences and Sherwood numbers for mass transfer. For example the diffusion rate for sodium hydroxide can be derived [8] assuming a chemically frozen boundary layer and using:

$$j_{\mathrm{NaOH}} = \frac{1}{M_{\mathrm{NaOH}}} \cdot \frac{Sh_{\mathrm{NaOH}}}{L} \cdot D_{\mathrm{NaOH}} \cdot N_{\mathrm{t,NaOH}} \cdot \varrho_{\mathrm{g}} \cdot ((w_{\mathrm{m,NaOH}} - w_{\mathrm{s,NaOH}}) + (\tau_{\mathrm{NaOH}}/N_{\mathrm{t,NaOH}}) \cdot w_{\mathrm{s,NaOH}}) \,. \qquad (5)$$

The Sherwood number *Sh* can be calculated analogous to the calculation of the Nusselt number. For the other components similar equations are used, describing the mass transfer per component directed towards or from the regenerator brick surfaces.

e) Checking the restrictions that:

- for no condensation: the net diffusivity rates of all sodium, all sulfur and all chloride components have to be zero;
- for sodium sulfate deposition: the total net diffusion rate of all sodium components has to be twice the net diffusion rate of all sulfur components, because in case of sodium sulfate for the deposition of two sodium atoms, one atom of sulfur is used and the net diffusion rate of all chlorides has to be zero.
  The total concentrations of sodium, sulfur and chloride in the flue gases at the refractory boundary will be adjusted and the calculation continues from step d).

f) After this iteration process, the deposition of sodium sulfate in this regenerator layer is calculated from the sodium and sulfur mass transfer rates.

g) The total amount of sodium and sulfur separation from the flue gas by deposition is calculated. By subtraction of the amounts condensed and deposited materials from the amounts present at the entrance of this regenerator layer, the remaining concentrations of sulfur, sodium and chloride compounds in the flue gases are determined.

h) The same calculation procedure will be used for the next layer in the regenerator.

At the end, the deposition and flue gas composition have been calculated as a function of the position in the regenerator. Figure 4 illustrates this deposition/condensation process. Dust formation in the flue gas takes place in the cooler sections of the checkers, this dust also diffuses partly to the refractory surfaces, causing additional deposition of fluffy salt layers. This process has been described in [11]. The dust, HCl and SO_x concentrations of the flue gases leaving the regenerators are also determined by this submodel.

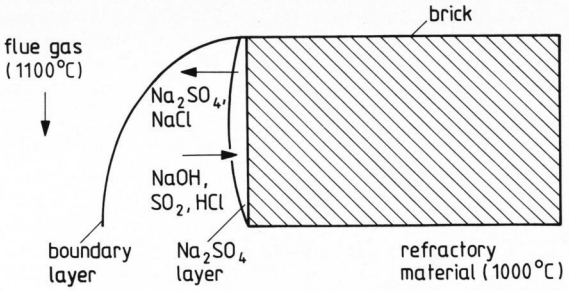

Figure 4. Deposition process in the regenerator of a soda–lime–silica glass furnace exemplarily shown by the sodium sulfate deposition.

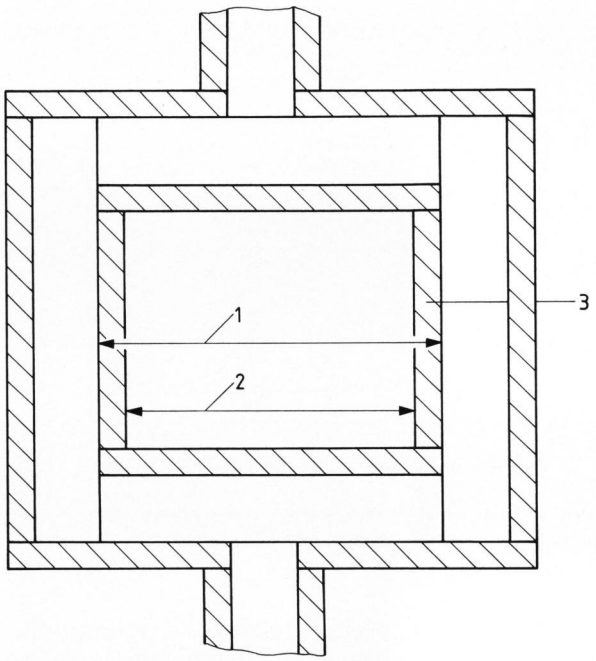

Figure 5. Change of flue gas channel dimensions by deposition layers in diagonally staggered packings. 1: original diameter, 2: actual diameter, 3: thickness of the deposition layer.

6. Combination of the four models

For a new glass furnace the calculation procedure starts with the input of data for the dimensions of the regenerator checkerworks and the packings, the thermal properties of the different refractory materials, glass furnace operation data, energy consumption data, air excess, batch composition and some other process data. A first assumption of the temperature of the flue gases entering the regenerator and an assumption of the temperatures of all the checkerwork layers is made. Then, as a first approach, the heat transfer from the flue gases to the packings as a function of time and layer position is calculated for the period of this half cycle of the combustion process.

After this step, the preheating of the air in the second half cycle is calculated. Using the values for the air-preheating temperature and an initial assumption for the crown temperatures of the furnace and assuming a certain combustion course, the thermal performance of the combustion chamber is calculated. This leads to corrected values for the temperatures in the furnace, for the flue gas temperatures and flue gas volume flows entering the regenerator. The regenerator calculation starts again, this procedure is continued until the exit flue gas and air-preheating temperatures become constant values. The thermal performance of the new furnace is now determined.

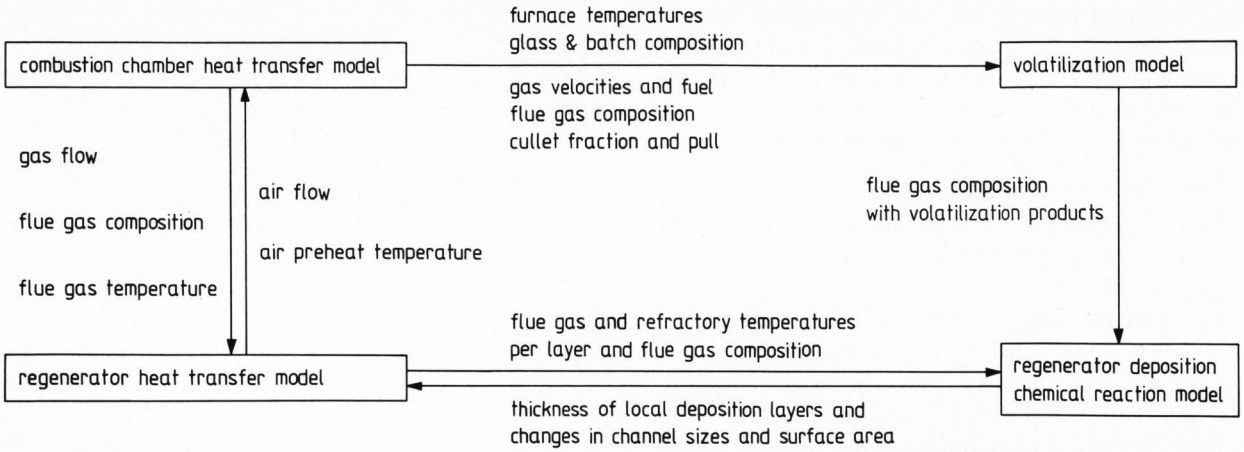

Figure 6. Coupling of submodels for determination of thermal behavior and aging of glass furnaces.

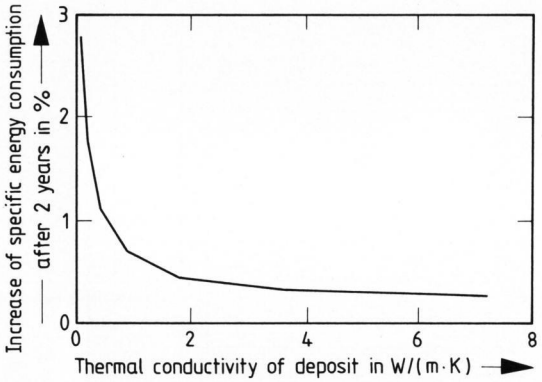

Figure 7. Change of specific energy consumption after 2 years depending on thermal conductivity of condensation products.

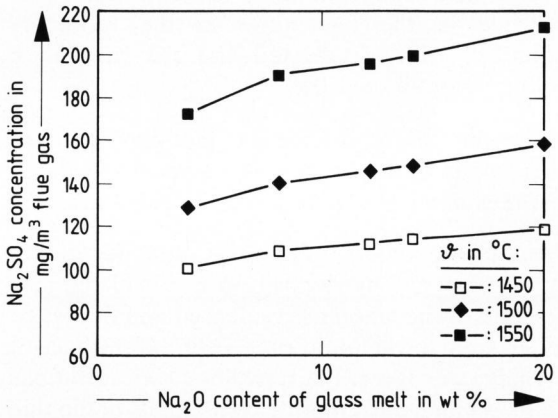

Figure 8. Dust concentration (Na_2SO_4) calculated as a function of sodium oxide content in the glass melt for 3 different temperatures.

From the batch composition, glass color (redox of the glass), flue gas velocities and temperatures determined by the combustion chamber model, the concentrations of sodium, sulfur and chlorides are calculated using the volatilization modeling (section 4.). The deposition rates in the regenerator are determined by the deposition model. Because of formation of the deposition layers the sizes of the flue gas channels become smaller, the surface areas of the checkerworks change and the effective thermal conduction of the packings decreases.

Regenerator heat transfer calculations are carried out after a certain period in which the deposition process took place, using adapted data that take the deposition per regenerator layer into account. The thermal conductivity changes and the channel width decreases. New air-preheating temperaturs are calculated and the heat transfer in the furnace is determined by the combustion chamber model. The procedure for the adaption of the new channel dimensions and specific surfaces is rather complex and depends on the kind of checkers. For several packings relations have been derived to calculate the changing dimensions of the channels due to the formation of deposition layers with a thickness, δ, depending on time and position. Figure 5 gives an illustration for the change of the packing dimensions. The coupling of the four submodels is presented by figure 6.

The thermal behavior and fouling can be determined as a function of time during the whole furnace lifetime. Intervals of 1 or 2 months are generally used for the calculation procedure of the fouling process and the change in thermal performance during the furnace lifetime.

7. Model calculations for different process conditions

Preliminary calculations show that the thermal conductivity of the sodium sulfate is essential for the aging process. From laboratory experiments with sodium sulfate deposits gathered from the cooler sections of an industrial glass furnace regenerator, the thermal conductivity for sodium sulfate dust has been determined to be approximately 0.1 to 0.4 W/(m K). These values can be applied for deposition layers

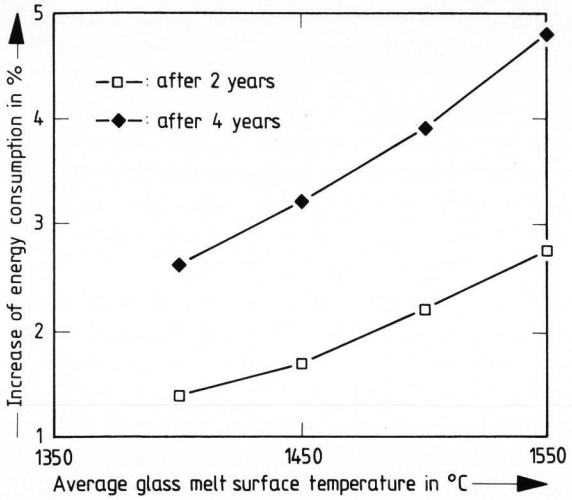

Figure 9. Decrease of thermal efficiency by deposition of sodium sulfate as a function of glassmelt surface temperature after 2 and 4 years.

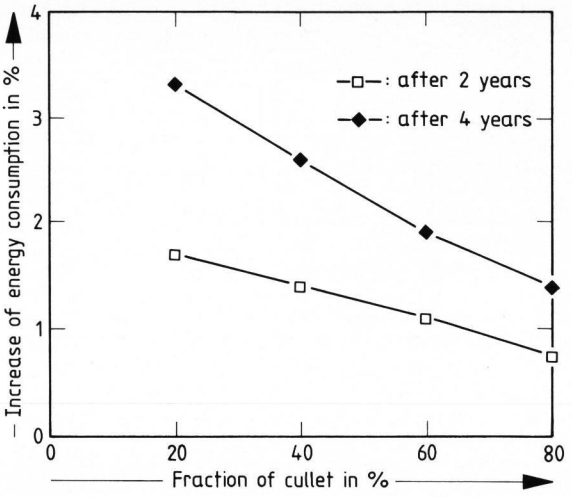

Figure 10. Effect of cullet fraction in batch on decrease of thermal efficiency of regenerative glass melting furnaces after 2 and 4 years.

below the sodium sulfate melting point of 884 °C, above this temperature a value of 1 W/(m K) has been assumed. The density below the melting point is determined to be approximately 1650 kg/m^3, above the melting point 2680 kg/m^3. Calculations with the model show the minor importance of the value of the heat capacity of the deposition layers.

Figure 7 shows the influence of thermal conductivity of sodium sulfate deposition layers on the increase of the specific energy consumption of a regenerative glass furnace after 2 years. From this it is clear that the fluffy sodium sulfate deposits with very low thermal conductivities result in strong aging effects. In the following some results of model calculations will be presented for a cross-fired furnace with diagonally staggered pigeonhole checkers using heavy oil as the main energy source.

7.1. Influence of temperature and sodium oxide concentration in the molten glass on aging and dust emissions

Figure 8 shows the influence of the sodium oxide concentration in the melt on the emissions of dust by the furnace at three temperatures of the molten glass surface, calculated from the volatilization and the combustion chamber model.

An increase of the sodium concentration in the glass leads to slight increases of the sodium sulfate dust emissions. The values for the calculated dust emissions for regenerative end-port soda–lime–silica glass furnaces are in a good agreement with emission measurements for similar industrial situations [12]. High melting temperatures result in very high volatilization and dust emission rates. This leads also to a very strong aging effect for the regenerators. The effect of the glassmelt surface temperature on the increase of the specific energy consumption after 2 and after 4 years of operation is given by figure 9.

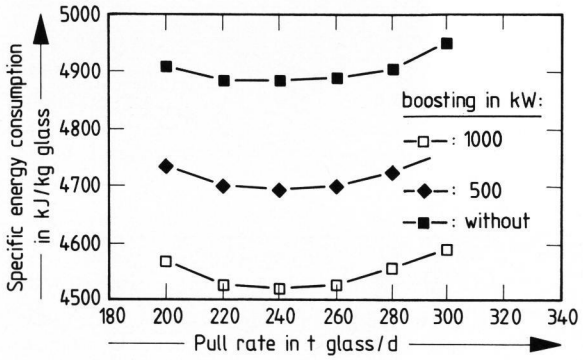

Figure 11. Influence of electrical boosting and pull rate on aging of regenerators after 2 years in a flint glass furnace with a melting area of 102 m^2.

7.2. Influence of cullet and electrical boosting on aging of the furnace performance

Furnaces which melt batches with high fractions of cullet have less batch carry-over and less sodium chloride volatilization from the soda. The aging of furnaces, using low amounts of cullet is much more pronounced compared to high cullet melters, as figure 10 shows.

Calculations including electrical boosting show that the aging decreases in the case that the electrical energy supply increases. Figure 11 shows the influence of electrical boosting and the pull rate on the change in thermal behavior of a glass furnace, producing flint glass in a tank with a surface area of 102 m^2. The aging is accelerated by higher pull rates as can be seen from these graphs. At high pull rates,

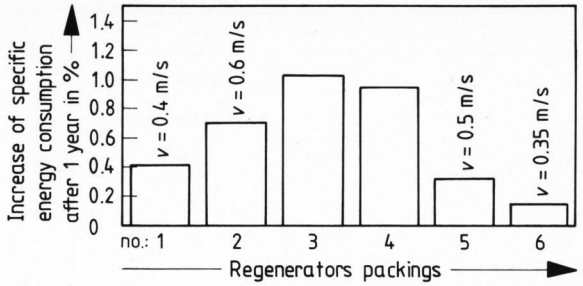

Figure 12. Aging and change in specific energy consumption for different flue gas velocities and the following regenerator packings: no. 1 and 2 – staggered pigeonhole, no. 3 – combined pigeonhole/basketweave packing I minor part: basketweave, no. 4 – combined pigeonhole/basketweave packing II major part: basketweave, no. 5 and 6 – chimney blocks.

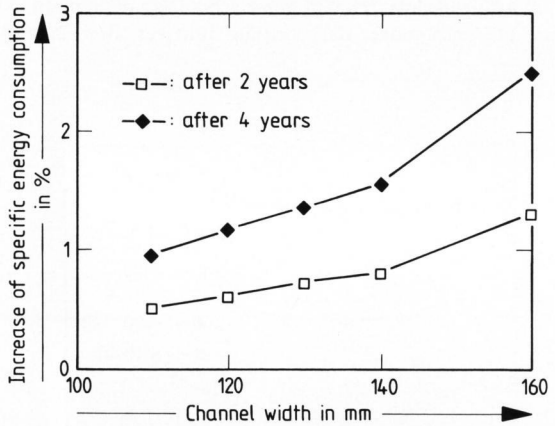

Figure 13. Change in energy consumption after 2 and 4 years depending on channel sizes in checkers made by chimney blocks.

flue gas velocities become very high, leading to high mass transfer rates. Thus, volatilization rates increase and so the deposition rates and the fouling in the checkerworks increase. For melters which use intensively electrical boosting, the aging of regenerators is moderate, because of the relatively low fossil fuel consumption, which gives lower flue gas velocities in the furnace and in the regenerators.

8. Results of calculations for different checkerworks

Calculations have been carried out for a regenerative furnace with different kinds of packings. The flue gas velocities have been changed for a few cases. Flue gas velocities between 0.35 and 0.6 m/s (referred to 273 K and 1013 mbar) have been used here. The aging, given as the increase of specific energy consumption after 1 year, has been derived for diagonally staggered pigeonhole packings, a combination of basketweave (top layers) and pigeonhole (lower layers) packing and chimney block checkers.

For a thermal conductivity of the deposition layers of 0.45 W/(m K), which is slightly higher than experimentally derived for sodium sulfate powder, 14 wt% Na_2O in the glass and a molten glass surface temperature of 1480 °C, the effect of aging on the energy consumption is given in figure 12. The staggered pigeonhole packing and the chimney blocks are less sensitive for fouling than the basketweave checkers. High glass pull rates, which give high flue gas velocities in the furnace and in the checkers, lead to severe aging of the regenerators.

As the channel width in the checkerworks decreases, the specific surface area (m^2 heat exchanging surface/m^3 checker) increases. The deposition is spread over a larger surface area for small channel sizes compared to wider channels and although the total deposition may increase, the deposition layer thickness remains relatively small for these situations. This means that the decrease in thermal efficiency of regenerators with small channels is less pronounced than for checkerworks with larger channel openings.

Figure 13 presents the calculated increase of the specific energy consumption after 2 and after 4 years for a chimney block packing as a function of the channel width.

9. Conclusions

The effect of the process conditions, the constructions of the regenerator checkerworks and the quality of the refractory materials used for the packings, on the change in thermal performance of glass furnaces can be derived quite accurately by using a coupling of four submodels, describing, first, the thermal behavior of regenerators, second, the combustion and radiative heat transfer in the glass furnace, third, the volatilization processes and fourth, the chemical reactions plus deposition in the regenerators.

Not only the thermal quality of a new regenerator can be determined, but also the thermal behavior after several years. Practical observations show that the increase of the specific energy consumption for industrial glass furnaces is about 1 to 3 %/year. Model calculations for several conditions show increases of 0.25 to 2 %/year, only by the effect of fouling by sodium sulfate deposition. Part of the decrease of the thermal efficiency of glass furnaces seems to be caused by corrosion or attack of the superstructure and aging of the insulation.

Chimney block packings and diagonally staggered pigeonhole checkers appear to be less sensitive for aging than basketweave arrangements. Wide channels may lead to a fast increase in energy consumption for the furnace, but, on the other hand, will reduce risks of channel blockages.

The model can be used to optimize regenerator design and for the choice of the regenerator packings, which could lead to average energy savings of 2 to 5 % during the furnace lifetime.

This research project has been carried out for the Arbeitsgemeinschaft industrieller Forschungsvereinigungen (AiF), Köln (FRG), which supported this work financially under the supervision of the Hüttentechnische Vereinigung der Deutschen Glasindustrie (HVG), Frankfurt/M. (FRG). The authors thank the companies PLM, Dongen (The Netherlands), and Flachglas AG, Gladbeck (FRG), for their cooperation in this study.

10. Nomenclature

10.1. Symbols

C_{pg}	the specific heat capacity of the flue gases in J/kg
C_{pr}	the specific heat capacity of the refractory material in J/kg
D	diffusivity of the gas in m/s^2
d_h	hydraulic diameter per channel in m
ΔF_s	heat-transferring surface area in layer i in m^2
j	molar flux in mol/(m^2 s)
k	mass transfer coefficient in m/s
L	characteristic length or distance in m
M	molar mass in kg/mol
N_t	correction parameter for thermophoretic diffusion
Q_s	heat flux density to or from refractory surface in J/(m^2 s)
Re	Reynolds number for the gas flow = $v \cdot d_h \cdot \varrho_g/\mu$
Sh	Sherwood number for mass transport = $k \cdot L/D$
$T_{fi}(t_j)$	flue gas or air temperature in layer i at time t_j in K
$T_{rsi}(t_j)$	refractory surface temperature of layer i at t_j in K
$T_{rci}(t_j)$	time-dependent temperature in the center of the brick in K
t_j	time in s
$\dot{V}$	flue gas volume flow in m^3/s
v	actual gas velocity in m/s
w	mass fraction in gas
α	heat transfer coefficient (including radiative, conductive and convective transfer) in J/(m^2 K s)
δ	thickness of regenerator brick in m
$\gamma(t_j)$	function derived from shape of temperature profile in refractory
μ	dynamic viscosity of gas in Pa s
ϱ	density in kg/m^3
τ	thermophoretic parameter given in [7]

10.2. Subscripts

c	center
f	flue gas
g	gaseous state
h	hydraulic
i	number of layer
j	time index
m	main gas flow
NaOH	referring to NaOH vapor
r	refractory
s	at surface position
t	thermophoretic diffusion

11. References

[1] Trier, W.: Glasschmelzöfen. Konstruktion und Betriebsverhalten. Berlin (et al.): Springer 1984.

[2] Barklage-Hilgefort, H.: Berechnung von Regeneratoren mit einem neuen numerischen Verfahren. Paper presented at the Technical Committee II of DGG on April 10, 1981 in Würzburg (FRG).

[3] Barklage-Hilgefort, H.: Wärmetechnische Messungen an Kammergitterungen. Glastech. Ber. **58** (1985) no. 4, p. 65–79.

[4] Hausen, H.: Wärmeübertragung in Gegenstrom, Gleichstrom und Kreuzstrom. 2nd ed. Berlin (et al.): Springer 1976.

[5] Schmalenbach, B.: Einfluß von Geschwindigkeiten und Strömungsverhalten auf den thermischen Wirkungsgrad von Regenerativkammern. In: Vorträge des XXVIII. Internationalen Feuerfest-Kolloquiums (XXVIIIth International Colloquium on Refractories), Aachen 1985. p. 248–262.

[6] VDI-Wärmeatlas. 4th ed. Düsseldorf: VDI-Verl. 1984.

[7] Beerkens, R. G. C.: Deposits and condensation from flue gases in glass furnaces. Univ. Technol. Eindhoven (The Netherlands), thesis 1986.

[8] Beerkens, R. G. C.; Waal, H. de: Simulation of the condensation and deposition processes in regenerators of glass furnaces. Glastech. Ber. **61** (1988) no. 2, p. 36–42.

[9] Conradt, R.; Scholze, H.: Zur Verdampfung aus Glasschmelzen. Glastech. Ber. **59** (1986) no. 2, p. 34–52.

[10] Manring, W. H.; Diken, G. M.: A practical approach to evaluating redox phenomena involved in the melting-fining of soda lime glasses. J. Non-Cryst. Solids **38 & 39** (1980) p. 813–818.

[11] Mutsaers, P. L. M.; Beerkens, R. G. C.; Waal, H. de: Fouling of heat exchanger surfaces by dust particles from flue gases of glass furnaces. Glastech. Ber. **62** (1989) no. 8, p. 266–273.

[12] Kircher, U.: Zur Problematik der gravimetrischen Staubemissionsmessung an Glasschmelzöfen. Glastech. Ber. **57** (1984) no. 8, p. 201–207.

92R0746